Austin Journal of Proteomics, Bioinformatics & Genomics

Open Access

Austin Publishing Group

Research Article

Interacting Network Analysis and Functional Profiling to Look Inside Adverse Ventricular Remodeling Post-Myocardial Infarction

Pietrovito L[1]*, Nguyen NT[2,3], Jin YF[2,3], Modesti PA[4], Lindsey ML[2,5,6] and Modesti A[1]

[1]Dipartimento di Scienze Biomediche, Sperimentali e Cliniche, Università degli Studi di Firenze, Italy

[2]San Antonio Cardiovascular Proteomics Center, University of Texas Health Science Center at San Antonio, USA

[3]Department of Electrical and Computer Engineering, University of Texas at San Antonio (UTSA), San Antonio, USA

[4]Dipartimento di Medicina Sperimentale e Clinica, Università degli Studi di Firenze, Italy

[5]Mississippi Center for Heart Research, Department of Physiology and Biophysics, University of Mississippi Medical Center,USA

[6]Research Service, G.V. (Sonny) Montgomery Veterans Affairs Medical Center, USA

***Corresponding author:** Pietrovito L, Dipartimento di Scienze Biomediche, Sperimentali e Cliniche,Viale G. Morgagni 50 50134, Università degli Studi di Firenze, Italy

Received: October 01, 2014; **Accepted:** February 21, 2015; **Published:** February 23, 2015

Abstract

Dysfunction of the left ventricle occurs to a varying degree in the most of surviving patients' post-myocardial infarction. In these patients, adverse remodeling frequently culminates in heart failure. Being able to predict patients who will progress to congestive heart failure would greatly advance in clinical prognostic capabilities.

The aim of this study was two-fold: to improve the knowledge on functional pathways of early and late left ventricleremodeling processes, and to generate new hypotheses to identify putative prognostic indicators for heart failure. To this purpose, we carried out a systems biology study using protein lists previously identified by proteomic studies.

Twenty-seven journal articles were included in our analysis. We generated two protein lists:a list of circulating proteins associated with adverse left ventricleremodeling (early changes); anda list of proteins found differentially expressed in ventricle tissue of patients with heart failure (later phase). We separately analyzed the protein sets by a combination of pioneering bioinformatics portals available on web.

We obtained significant enrichments of blood proteins involved in extracellular matrix remodeling, collagen catabolism, response to stress, and the inflammatory response, while the alterations in the left ventricle reflected remarkable activation of the respiratory chain coupled with ATP production and oxidative metabolism. We provided new insights into the pathogenesis of adverse ventricularremodeling and heart failure and we brought to light some intermediate proteins likely involved in the disease mechanisms not previously associated with the failing status, supplying a new rationale for drug development and further discovery of biomarkers of these heart pathologies.

Keywords: Proteomics; Ventricular Remodeling; Heart Failure; Systems Biology; Matrix Metalloproteinase; Respiratory chain

Abbreviations

LV: Left Ventricle; HF: Heart Failure; MI: Myocardial Infarction; LVSD: Left Ventricular Systolic Dysfunction; ICM: Ischemic Cardiomyopathy; ORA: Over-Representation Analysis; BP: Biological Process; MF: Molecular Function; CC: Cellular Component; ECM: Extracellular Matrix; BPLVR: Blood Proteins List from Patients with Adverse Remodeling Post-MI; LVTP: LV Tissue Proteins List From Patients with HF

Introduction

Adverse remodelingof the left ventricle (LV) defines a pathological process during which molecular, biochemical, and cellular changes lead to alterations in shape, dimensions, and function of the LV. This cascade of eventsincludes dilatation, hypertrophy, and the formation of a discrete collagen scar anditcan occur in response to different conditions including myocardial infarction (MI), pressure overload (hypertension), volume overload (valvular heart disease) or cardiomyopathy [1]. Following MI, the remodeling response begins within hours after the ischemic insult and can continue for months, even years, involving both the infarcted and non-infarcted regions of the LV. The remodelingprocess persists until a balance has been reached between the distention forces generated following the dilatation of the ventricle chamberand the traction forces exerted by the collagen scar [2]. If the adaptive response fails, progressive dilatation and fibrosis will provoke extensive worsening of LV function until develop into HF [3].

Although persistent cardiac remodeling is widely accepted to be associated with high risk of HF and death, the early diagnosis of remodeling has only recently been appreciated as a pivotal time for intervention.Deriving new insights into the temporal evolution and biochemical pathways that drive LV remodeling representsa current challenge in efforts toreduce the mortality, morbidity, and the costs of HF.Unfortunately,adverse LVremodeling is a compensatory mechanism that often progresses without obvious changes in the collected clinical variables[4]. Wang and colleagues recently reported that the incidence of asymptomatic left ventricular systolic dysfunction

Citation: Pietrovito L, Nguyen NT, Jin YF, Modesti PA, Lindsey ML and Modesti A. Interacting Network Analysis and Functional Profiling to Look Inside Adverse Ventricular Remodeling Post-Myocardial Infarction. Austin J Proteomics Bioinform & Genomics. 2015;2(1): 1007.

Table 1: List of BPLVR and main clinical features of the studies selected from literature.

Protein Name	AN[a]	Time of Sampling [b]	Change in Circulating Level Post-MI	AMI cohort[d]				Ref.[e]
				Cnt[c]	Mean age	Sex (male %)	No. of Patients	
Adiponectin	Q15848	1 d	"-	†	55	NS	75	[7]
Apelin	Q9ULZ1	12h-2 d; 6 mo	"- / -	#	59	77	100	[8]
Atrial natriuretic peptide (ANP)	P01160	12 h, 1, 3 mo	"+ / + /+	#	59	76	33	[9]
		2 d; 1, 2 wk; 1 mo	"+ / + / + / +	#	61	73	30	[10]
Brain natriuretic peptide (BNP)	P16860	12h, 1, 3 mo	"+ / + /+	#	59	76	33	[9]
		2 d; 1, 2 wk; 1 mo	"+ / + / + / +	#	61	73	30	[10]
		1 mo	"+	§	63	72	246	[11]
		1 d	"+	†	63	80	97	[12]
		46 h; 3, 6 mo	"+ / + / =	†	59	77	100	[13]
C-reactive protein (CRP)	P02741	1 d	"-	†	55	NS	75	[7]
		1-3 d	"+	†	58	50	35	[14]
		2 d; 1 wk; 2 mo; 1 y	"- / - / = / =	†	59	81	42	[15]
		3 d; 1 wk; 6 mo	"+ / + / +	#	57	63	75	[16]
		12 h; 5 d	"+ / +	§	59	NS	30	[17]
Fas ligand	Q53ZZ1	1 mo	"+	§	63	72	246	[11]
Ferritin	P02792	1-3 d	"-	†	64	71	258	[18]
Growth differentiation factor 15 (GDF15)	Q99988	1 d	"+	†	63	80	97	[12]
		2 d; 1 wk; 2 mo; 1 y	"- / - / - / -	†	59	81	42	[15]
Interleukin-1 (IL-1) receptor-like 1, soluble isoform (ST2)	Q01638	46 h; 3, 6 mo	"+ / + / +	§	59	77	100	[19]
		1 d; 2 wk; 3 mo	“+ / = / =	§	61	78	69	[20]
		1 d-1 mo	"+	†	58	80	1239	[21]
Interleukin-10 (IL-10)	P22301	3 d; 1 wk; 6 mo	"+ / + / +	#	57	63	75	[16]
Interleukin-18 (IL-18)	Q14116		"+	#	55	74	399	[22]
Interleukin-3 (IL-3)	P08700	12 h; 5 d	"+ / +	§	59	NS	30	[17]
Interleukin-6 (IL-6)	P05231	3 d; 1 wk; 6 mo	"+ / + / +	#	57	63	75	[16]
Macrophage colony-stimulating factor 1 (CSF-1)	P09603	12 h; 5 d	"+ / +	§	59	NS	30	[17]
Macrophage inflammatory protein-1 alpha (MIP-1α)	P10147	1-7 d; 1 mo	"+ / +	†	58	50	35	[14]
Matrix metalloproteinase-1 (MMP-1)	P03956	3-7 d; 1, 3 mo; 1 y	"= / = / = / =	§	57	81	239	[23]
Matrix metalloproteinase-2 (MMP-2)	P08253	46 h; 3, 6 mo	"= / = / =	†	59	77	100	[13]
		3-7 d; 1, 3 mo; 1 y	“-/ +/ +/ +	§	57	81	239	[23]
		1, 3 d; 1 wk; 1 mo	"- / + / + / +	§	63	83	108	[24]
		2, 5 d; 1, 3, 6 mo	"- / - / - / - / -	#	58	75	32	[25]
		12 h; 1, 2, 3, 4 d; 6 mo	"+ / + / + / + / + / +	†	63	73	91	[26]
		1, 2, 3, 4, 5 d	"+ / + / + / = / =	§	63	75	60	[27]
Matrix metalloproteinase-3 (MMP-3)	P08254	46 h; 3, 6 mo	"+ / = / =	†	59	77	100	[13]
		3-7 d; 1, 3 mo; 1 y	"- / + / + / +	§	57	81	239	[23]
		12 h; 1, 2, 3, 4 d	"+ / + / + / + / +	†	64	74	382	[28]
Matrix metalloproteinase-7 (MMP-7)	P09237	2, 5 d; 1, 3, 6 mo	"+ / + / = / = / =	#	58	75	32	[25]
Matrix metalloproteinase-8 (MMP-8)	P22894	3-7 d; 1, 3 mo; 1 y	"+ / - / - / -	§	57	81	239	[23]
		2, 5 d; 1, 3, 6 mo	"+ / = / = / = / =	#	58	75	32	[25]
Matrix metalloproteinase-9 (MMP-9)	P14780	46 h; 3, 6 mo	"- / - / -	†	59	77	100	[13]
		3-7 d; 1, 3 mo; 1 y	"+ / - / + / -	§	57	81	239	[23]
		1, 3 d; 1 wk; 1 mo	"+ / - / - / -	§	63	83	108	[24]
		2, 5 d; 1, 3, 6 mo	"+ / + / + / + / +	#	58	75	32	[25]
		12 h, 1, 2, 3, 4 d; 6 mo	+ / = / = / = / = / =	†	63	73	91	[26]
		1, 2, 3, 4, 5 d	"+ / = / = / + / =	§	63	75	60	[27]
Monocyte chemoattractant protein-1 (MCP-1)	P13500	2 d; 3, 6 mo	"+ / + / +	†	59	77	100	[13]
		1-7 d; 1 mo	"+ / +	†	58	50	35	[14]
Myocardial connective tissue growth factor (CTGF)	P29279	2 d; 1 wk; 2 mo; 1 y	"+ / + / + / +	†	59	81	42	[15]
Pterin-4-alpha-carbinolamine dehydratase	P61457	1 d	"+	†	64	85	108	[29]
T-cell-specific protein RANTES	P13501	1-7 d; 1 mo	"+ / +	†	58	50	35	[14]
TGF-beta receptor type-1 (TGFBR1)	P36897	12 h	"+	†	56	85	115	[30]
Tissue inhibitor of metalloproteinase-1 (TIMP-1)	P01033	3-7 d; 1, 3 mo; 1 y	"+ / - / - / -	§	57	81	239	[23]
		1, 3 d; 1 wk; 1 mo	"+ / + / - / -	§	63	83	108	[24]
		2, 5 d; 1, 3, 6 mo	"+ / + / + / = / =	#	58	75	32	[25]
		1, 2, 3, 4, 5 d	"= / = / = / + / =	§	63	75	60	[27]
Tissue inhibitor of metalloproteinase-2 (TIMP-2)	P16035	3-7 d; 1, 3 mo; 1 y	"- / + / + / +	§	57	81	239	[23]
		2, 5 d; 1, 3, 6 mo	"= / + / + / + / +	#	58	75	32	[25]
Tissue inhibitor of metalloproteinase-4 (TIMP-4)	Q99727	3-7 d; 1, 3 mo; 1 y	"- / + / + / +	§	57	81	239	[23]
		2, 5 d; 1, 3, 6 mo	"= / + / + / + / +	#	58	75	32	[25]
Tissue plasminogen activator (t-PA)	P00750	46 h; 3, 6 mo	"+ / = / =	†	59	77	100	[13]
Transforming growth factor beta-1 (TGF-ß1)	P01137	12 h	"+	†	56	85	115	[30]
Tumor necrosis factor (TNF- α)	P01375		"+	#	55	74	399	[22]
Vasopressin-neurophysin 2-copeptine	P01185	1, 3, 5 d	"+ / = / =	§	66	80	980	[31]
		3, 5 d	"+ / +	§	59	77	274	[32]
von Willebrand factor (vWf)	P04275	46 h; 3, 6 mo	= / = / =	†	59	77	100	[13]

[a] AN= Accession Number in Swiss-Prot Protein database

[b]Time of blood collection post-MI

[c] Control subjects age- and sex-matched recruited into the study: # Healthy subjects, † Patients with preserved LV function post-MI, § Comparison into the same group of patients post-MI (considering others correlation factors e.g. anterior AMI *vs* inferior AMI)

[d]Baseline characteristics of acute myocardial infarction patients

[e] References

(LVSD) in the community ranges from 3% to 6%, though as common as systolic HF but often occurring without known cardiovascular diseases[5].Currently, first screening of patients with known or suspected myocardial dysfunction is achieved by electrocardiography, cardiac imaging, and blood chemistry. However, each measure screened for cardiac remodelingpresents some limitations and it is indicative of a different aspect of the disease,without providing a comprehensive picture of the pathological state.

Systems biology, through the identification of the biological networks connecting the different molecular elements, may supply new powerful insights into the pathogenesis of complex diseases [6]. In particular, by combining the systems biology approach to a bioinformatics analysis, it is possible to identifythe protein-protein interactionsnetworks and their functional enrichments, thus vastly improving the knowledge on the central biological mechanisms of the disease.

In the current study, we performed an extensive systems biology analysis of human adverse LV remodeling by functional profiling and network analysis to improve the understanding on functional pathways of the early and late LV remodeling process and to provide novel hypotheses on likely prognostic indicators, with the final goal to improve the treatment of adverse cardiac remodeling and HF.Ourstudy was focused on two different systems: blood and LV tissue. We generated two different protein lists based on the type of the examined sample and we started the analysis with the list of blood proteins previously associated with adverse left ventricular remodeling (BPLVR)[7-32]. Subsequently, we uploaded the list of LV proteins found differentially expressed in patients with congestive HF triggered by ischemic cardiomyopathy (ICM) in comparison with healthy tissues[33]. The collected data were analysed using a combination of over-representation analysis (ORA) tools available as Cytoscape apps or as web-based portals (www.bioprofiling.de and bioinfo.vanderbilt.edu/webgestalt/) [34-36].

Methods

Data collection

We performed a Medline search by using individually or in combination the following criteria: “proteomics”, “adverse remodeling”, “heart failure”, “serological biomarkers”, and “human ventricular tissue”.The search was time-restricted to November, 2013.

Concerning the association between circulating proteins and adverse remodeling, we focused on changes that occurred during the first month post-MI (early alterations). We considered only cohort studies or clinical trials carried out with at least 30 patients admitted with acute MI (AMI). The blood proteins considered in our study, their Swiss-Prot Protein database accession numbers, the main features of the twenty-six publications and the relative references [7-32] considered are displayed in table 1.

The complete list of the LV tissue proteins (LVTP) is reported in tableS1. To our knowledge, the proteomic profile of LV tissue from patients with HF triggered by MI was reported only in one recently published paper by Roselló-Lletí[33].We selected the LV proteins found differentially expressed in patients with congestive HF triggered by ischemic cardiomyopathy (ICM) in comparison with healthy tissues and we excluded the proteins whose modifications in expression levels were caused by dilated cardiomyopathy (DCM).

Bioinformatics and statistical analysis

TheORA of the two input lists (Tables 1, S1)was carried out using the WebGestalt online tools (http://bioinfo.vanderbilt.edu/webgestalt/) [34].WebGestalt is a bioinformatics platform designed for functional genomics, proteomics and large-scale genetic studies from which large number or genes/proteins are continuously generated.The program manages supports and uses data from multiple different databases, such as GO, IntAct, Reactome, KEGG, Pathway Commons and WikiPathways. In WebGestalt, following the upload of the input list, the user can choose the type of analysis to perform. The current version of WebGestalt covers eight organisms including human, mouse, yeast and zebrafish, and it is able to analyze the uploaded list for functional enrichments in various biological contexts.

To obtain functional advanced enrichments and to build interacting networks of the submitted protein lists we used the web portal BioProfiling de(www.bioprofiling.de) [35].Bioprofiling.de is an easy tool of analysis for the interpretation of lists of genes/proteins. The program accepts a directory of Accesion Number (AN) as input and provides a list of genes as output.For this study, we used three different BioProfilingapplications: (i) ProfCom_GO, (ii) PPI spider and (iii) R spider [43]. ProfComGO wasused for functional profiling. The output of ProfCom_GOis a list of enriched “complex classes”. Such classes, in general characterized by a more specific biological function compared to the single GO terms, are constructed by combination of three Boolean operations: intersection, union and difference (“OR”, “AND”, and “NOT”) of available functional terms within GO and FunCat databases and enriched in input protein list.

PPI and R spider are two tools of BioProfiling pipeline able to provideenriched protein maps. of the submitted list. PPI spider is based on protein-protein interactions networks derived from IntAct, while R spider uses a combination of signaling and metabolic pathways from Reactome and KEGG databases. Both programs profile the protein networks according to three different models. In model D1, the networks were built only considering the direct interactions between the input proteins, while in the models D2 and D3 one or two intermediate nodes were added. The significant enrichments provided by BioProfiling were determined with the default parameter settings. The p-value presented, computed by Monte Carlo simulation (http://www.bioprofiling.de/statistical_frameworks.html), referred to the probability of obtaining a model of the same quality for a random gene list of the same size.

Visualization with cytoscape

The significant enriched networks (p-value < 0.01) were exported as an ‘xgmml’ file and visualized by Cytoscape 3.1.0 (http://www.cytoscape.org/), aopen-source software for the large-scale integration of interaction network data [36].

Results and Discussion

Bioinformatics analysis of the blood proteins list from patients with adverse remodeling post-MI (BPLVR)

At first we analysed theinputlist of circulating proteins (Table1) by using WebGestalt resources, in order to obtain the ORA of

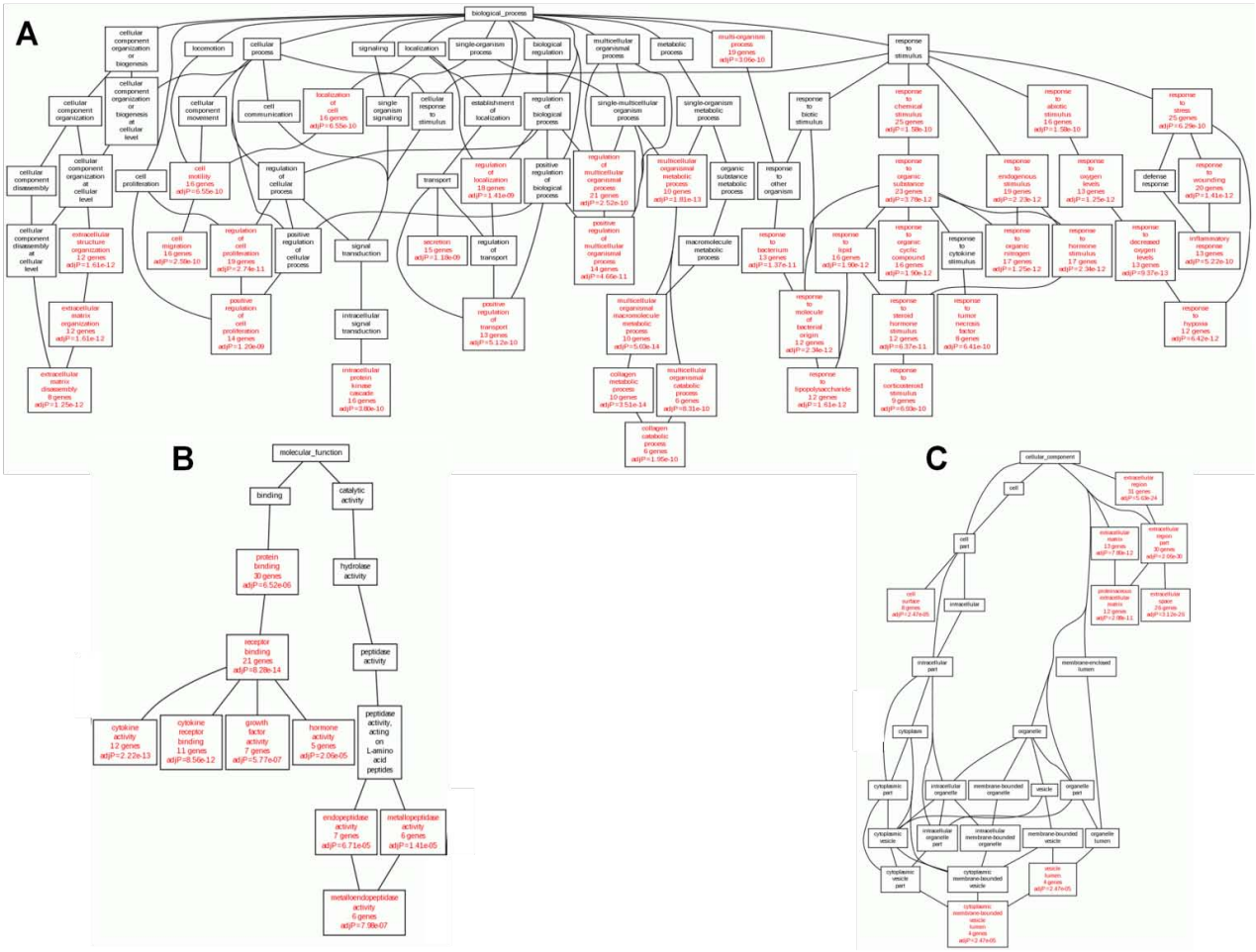

Figure 1: Over-representation analysis of GO categories in BPLVR. The analysis with Web Gestalt disclosed functional GO enrichments grouped according to Biological Process (A), Molecular Function (B), and Cellular Component (C). GO terms in red are the enriched GO categories, while the black ones are their non-enriched parents. Each node shows the name of the GO category, the number of genes in the category and the adjusted p-value indicating the significance of enrichment.

proteomics data. Moreover, toincrease the specificity of the functional enrichments and the number of putative proteins associated with the disease, we subsequently uploaded the input liston BioProfiling.de.

GO over-representation analysis

Figure 1 reports the GO Treesrelated to Biological Process (BP, Panel A), Molecular Function (MF, Panel B) and Cellular Component (CC, Panel C)classes obtained after performing the ORA of GO categories by the Webgestalt portal. In BP sub-root are present40 enriched GO categories. As expected,during the first month post-MI there was a significant increase in circulating levels of proteins involved in 'response to stress' (GO:0006950 – 25 proteins), 'response to wounding' (GO:0009611 - 20 proteins), 'inflammatory response' (GO:0006954 – 13 proteins), 'response to decreased oxygen levels' (GO:0036293 – 13 proteins) and 'response to hypoxia' (GO:0001666 – 12 proteins). The bioinformatics analysis also revealed enrichments of proteins implicated in 'regulation of cell proliferation' (GO:0042127 - 19 proteins) and 'cell migration' (GO:0016477 – 16 proteins). However, the key enrichments werethose ofproteins engaged in 'extracellular matrix disassembly' (GO:0022617 – 8 proteins) and 'collagen catabolic process' (GO:0030574 – 6 proteins). In fact, despite the number of proteins belonging to these categories has been relatively small compared to the entire submitted list, the values of the enrichment ratios were extremely high (full reports of enriched GO categories of circulating biomarkers provided by WebGestalt are available in table S2). Concerning the MF sub-root, it included five ontologies involved in protein binding: 'receptor binding'(GO:0005102 - 21 proteins), 'cytokine activity' (GO:0005125 – 12 proteins), 'cytokine receptor binding' (GO:0005126 - 11 proteins), 'growth factor activity' (GO:0008083 - 7 proteins),and 'hormone activity' (GO:0005179 - 5 proteins). Moreover, in accordance with the BP categories, the MF enrichmentswere related to 'metalloendopeptidase activity' (GO:0004222 –7 proteins), and 'endopeptidase activity' (GO:0004175 – 7 proteins). Finally, the CCpanel revealed that 31 proteins of the input list (more than 90%) localize in 'extracellular region' (GO:0005576). More in detail, 13 proteins pinpointed in 'ECM' (GO:0031012), 8 proteins in 'cell surface' (GO:0009986) and 4 proteins in 'cytoplasmic membrane-bounded vescicle lumen' (GO:0060205). The set of blood proteinswas then analyzed with respect to theKEGG, PathwayCommons, and Wikipathways databases (Table 2). The entries provided by KEGG pathways disclosed significant enrichments of proteins common to other pathologies, including

Table 2: Over-representation of enriched categories in BPLVR list provided by using KEGG(A),PathwayCommons(B)andWikipathways (C)databases. pvalue < 0.0001 after Benjamini-Hochberg correction.

Pathway Name	#[a]	AN[b]	Statistics[c]
(A) KEGG pathways			
Rheumatoid arthritis	10	P01137 P01375 P08254 P13500 P05231 P09603 P03956 Q14116 P10147 P13501	C=91; O=10; E=0.07; R=139.39; rawP=1.32e-19; adjP=1.58e-18
Cytokine-cytokine receptor interaction	12	P01137 P01375 P08700P13500P05231 P09603 Q53ZZ1Q14116P36897P10147P22301P13501	C=265; O=12; E=0.21; R=57.44; rawP=1.10e-18; adjP=6.60e-18
Chagas disease (American trypanosomiasis)	9	P01137 P01375 P13500 P05231 Q53ZZ1P36897P10147P22301P13501	C=104; O=9; E=0.08; R=109.77; rawP=9.65e-17; adjP=3.86e-16
Malaria	6	P01137 P01375 Q14116P22301P13500P05231	C=51; O=6; E=0.04; R=149.23; rawP=2.64e-12; adjP=7.92e-12
African trypanosomiasis	5	Q53ZZ1P01375 Q14116P22301P05231	C=35; O=5; E=0.03; R=181.21; rawP=7.15e-11; adjP=1.72e-10
NOD-like receptor signaling pathway	5	P01375 Q14116P13501P13500P05231	C=58; O=5; E=0.05; R=109.35; rawP=9.96e-10; adjP=1.99e-09
Pathways in cancer	7	Q53ZZ1P03956 P14780P01137P36897P05231P08253	C=326; O=7; E=0.26; R=27.24; rawP=5.97e-09; adjP=1.02e-08
Hematopoietic cell lineage	4	P01375 P08700P05231P09603	C=88; O=4; E=0.07; R=57.66; rawP=7.16e-07; adjP=1.07e-06
Toll-like receptor signaling pathway	4	P01375 P10147P13501P05231	C=102; O=4; E=0.08; R=49.74; rawP=1.29e-06; adjP=1.72e-06
Amoebiasis	4	P01137P01375 P22301P05231	C=106; O=4; E=0.08; R=47.87; rawP=1.51e-06; adjP=1.81e-06
Osteoclast differentiation	4	P01137P01375 P36897P09603	C=128; O=4; E=0.10; R=39.64; rawP=3.20e-06; adjP=3.49e-06
MAPK signaling pathway	4	Q53ZZ1P01137P01375 P36897	C=268; O=4; E=0.21; R=18.93; rawP=5.84e-05; adjP=5.84e-05
(B) PathwaysCommons			
ErbB1 downstream signaling	20	P08700P01375P01137P14780P13500P01160P03956P36897Q99988P22301P13501P09237P08254P01033P29279P09603P05231P08253Q53ZZ1P02741	C=1288; O=20; E=1.02; R=19.70; rawP=2.58e-22; adjP=6.90e-22
PAR1-mediated thrombin signaling events	20	P08700P01375P01137P14780P13500P01160P03956Q99988P36897P22301P13501P09237P29279P01033P08254P09603P05231P08253Q53ZZ1P02741	C=1299; O=20; E=1.02; R=19.53; rawP=3.05e-22; adjP=6.90e-22
VEGF and VEGFR signaling network	20	P08700P01375P01137P14780P13500P01160P03956Q99988P36897P22301P13501P09237P29279P01033P08254P09603P05231P08253Q53ZZ1P02741	C=1304; O=20; E=1.03; R=19.45; rawP=3.29e-22; adjP=6.90e-22
S1P1 pathway	20	P08700P01375P01137P14780P13500P01160P03956Q99988P36897P22301P13501P09237P29279P01033P08254P09603P05231P08253Q53ZZ1P02741	C=1288; O=20; E=1.02; R=19.70; rawP=2.58e-22; adjP=6.90e-22
PDGF receptor signaling network	20	P08700P01375P01137P14780P13500P01160P03956Q99988P36897P22301P13501P09237P29279P01033P08254P09603P05231P08253Q53ZZ1P02741	C=1293; O=20; E=1.02; R=19.62; rawP=2.79e-22; adjP=6.90e-22
Nectin adhesion pathway	20	P08700P01375P01137P14780P13500P01160P03956Q99988P36897P22301P13501P09237P29279P01033P08254P09603P05231P08253Q53ZZ1P02741	C=1295; O=20; E=1.02; R=19.59; rawP=2.87e-22; adjP=6.90e-22
Urokinase-type plasminogen activator (uPA) and uPAR-mediated signaling	20	P08700P01375P01137P14780P13500P01160P03956Q99988P36897P22301P13501P09237P29279P01033P08254P09603P05231P08253Q53ZZ1P02741	C=1288; O=20; E=1.02; R=19.70; rawP=2.58e-22; adjP=6.90e-22
Signaling events mediated by VEGFR1 and VEGFR2	20	P08700P01375P01137P14780P13500P01160P03956Q99988P36897P22301P13501P09237P29279P01033P08254P09603P05231P08253Q53ZZ1P02741	C=1296; O=20; E=1.02; R=19.57; rawP=2.92e-22; adjP=6.90e-22
LKB1 signaling events	20	P08700P01375P01137P14780P13500P01160P03956Q99988P36897P22301P13501P09237P29279P01033P08254P09603P05231P08253Q53ZZ1P02741	C=1308; O=20; E=1.03; R=19.40; rawP=3.50e-22; adjP=6.90e-22
Alpha9 beta1 integrin signaling events	20	P08700P01375P01137P14780P13500P01160P03956Q99988P36897P22301P13501P09237P29279P01033P08254P09603P05231P08253Q53ZZ1P02741	C=1305; O=20; E=1.03; R=19.44; rawP=3.34e-22; adjP=6.90e-22
Syndecan-1-mediated signaling events	20	P08700P01375P01137P14780P13500P01160P03956Q99988P36897P22301P13501P09237P29279P01033P08254P09603P05231P08253Q53ZZ1P02741	C=1300; O=20; E=1.02; R=19.51; rawP=3.10e-22; adjP=6.90e-22
Class I PI3K signaling events	20	P08700P01375P01137P14780P13500P01160P03956Q99988P36897P22301P13501P09237P29279P01033P08254P09603P05231P08253Q53ZZ1P02741	C=1288; O=20; E=1.02; R=19.70; rawP=2.58e-22; adjP=6.90e-22
Endothelins	20	P08700P01375P01137P14780P13500P01160P03956Q99988P36897P22301P13501P09237P29279P01033P08254P09603P05231P08253Q53ZZ1P02741	C=1307; O=20; E=1.03; R=19.41; rawP=3.45e-22; adjP=6.90e-22
Internalization of ErbB1	20	P08700P01375P01137P14780P13500P01160P03956Q99988P36897P22301P13501P09237P29279P01033P08254P09603P05231P08253Q53ZZ1P02741	C=1288; O=20; E=1.02; R=19.70; rawP=2.58e-22; adjP=6.90e-22
IL5-mediated signaling events	20	P08700P01375P01137P14780P13500P01160P03956Q99988P36897P22301P13501P09237P29279P01033P08254P09603P05231P08253Q53ZZ1P02741	C=1292; O=20; E=1.02; R=19.64; rawP=2.74e-22; adjP=6.90e-22

Glypican 1 network	20	P08700P01375P01137P14780P13500P01160P03956Q99988P36897P22301P13501P09237P29279P01033P08254P09603P05231P08253Q53ZZ1P02741	C=1299; O=20; E=1.02; R=19.53; rawP=3.05e-22; adjP=6.90e-22
Thrombin/protease-activated receptor (PAR) pathway	20	P08700P01375P01137P14780P13500P01160P03956Q99988P36897P22301P13501P09237P29279P01033P08254P09603P05231P08253Q53ZZ1P02741	C=1300; O=20; E=1.02; R=19.51; rawP=3.10e-22; adjP=6.90e-22
GMCSF-mediated signaling events	20	P08700P01375P01137P14780P13500P01160P03956Q99988P36897P22301P13501P09237P29279P01033P08254P09603P05231P08253Q53ZZ1P02741	C=1292; O=20; E=1.02; R=19.64; rawP=2.74e-22; adjP=6.90e-22
Plasma membrane estrogen receptor signaling	20	P08700P01375P01137P14780P13500P01160P03956Q99988P36897P22301P13501P09237P29279P01033P08254P09603P05231P08253Q53ZZ1P02741	C=1301; O=20; E=1.03; R=19.50; rawP=3.15e-22; adjP=6.90e-22
Arf6 signaling events	20	P08700P01375P01137P14780P13500P01160P03956Q99988P36897P22301P13501P09237P29279P01033P08254P09603P05231P08253Q53ZZ1P02741	C=1288; O=20; E=1.02; R=19.70; rawP=2.58e-22; adjP=6.90e-22
Arf6 trafficking events	20	P08700P01375P01137P14780P13500P01160P03956Q99988P36897P22301P13501P09237P29279P01033P08254P09603P05231P08253Q53ZZ1P02741	C=1288; O=20; E=1.02; R=19.70; rawP=2.58e-22; adjP=6.90e-22
PDGFR-beta signaling pathway	20	P08700P01375P01137P14780P13500P01160P03956Q99988P36897P22301P13501P09237P29279P01033P08254P09603P05231P08253Q53ZZ1P02741	C=1288; O=20; E=1.02; R=19.70; rawP=2.58e-22; adjP=6.90e-22
Insulin Pathway	20	P08700P01375P01137P14780P13500P01160P03956Q99988P36897P22301P13501P09237P29279P01033P08254P09603P05231P08253Q53ZZ1P02741	C=1288; O=20; E=1.02; R=19.70; rawP=2.58e-22; adjP=6.90e-22
EGFR-dependent Endothelin signaling events	20	P08700P01375P01137P14780P13500P01160P03956Q99988P36897P22301P13501P09237P29279P01033P08254P09603P05231P08253Q53ZZ1P02741	C=1289; O=20; E=1.02; R=19.68; rawP=2.62e-22; adjP=6.90e-22
Arf6 downstream pathway	20	P08700P01375P01137P14780P13500P01160P03956Q99988P36897P22301P13501P09237P29279P01033P08254P09603P05231P08253Q53ZZ1P02741	C=1288; O=20; E=1.02; R=19.70; rawP=2.58e-22; adjP=6.90e-22
IL3-mediated signaling events	20	P08700P01375P01137P14780P13500P01160P03956Q99988P36897P22301P13501P09237P29279P01033P08254P09603P05231P08253Q53ZZ1P02741	C=1295; O=20; E=1.02; R=19.59; rawP=2.87e-22; adjP=6.90e-22
Signaling events mediated by Hepatocyte Growth Factor Receptor (c-Met)	20	P08700P 01375P01137P1 4780P13500P01160P03 956Q99988P36897 P22301P13501P09237 P29279P01033P0825 4P09603P05231P08253Q 53ZZ1P02741 P08700P01375P01137P14 780P13500P0 1160P03956Q99988P36897 P22301P13501P09237 P29279P01033P08254P09603P05231P08253 Q53ZZ1P02741	C=1293; O=20; E=1.02; R=19.62; rawP=2.79e-22; adjP=6.90e-22
IFN-gamma pathway	20	P08700P01375P01137P14780P13500P01160P03956Q99988P36897P22301P13501P09237P29279P01033P08254P09603P05231P08253Q53ZZ1P02741	C=1296; O=20; E=1.02; R=19.57; rawP=2.92e-22; adjP=6.90e-22
Signaling events mediated by focal adhesion kinase	20	P08700P01375P01137P14780P13500P01160P03956Q99988P36897P22301P13501P09237P29279P01033P08254P09603P05231P08253Q53ZZ1P02741	C=1288; O=20; E=1.02; R=19.70; rawP=2.58e-22; adjP=6.90e-22
EGF receptor (ErbB1) signaling pathway	20	P08700P01375P01137P14780P13500P01160P03956Q99988P36897P22301P13501P09237P29279P01033P08254P09603P05231P08253Q53ZZ1P02741	C=1288; O=20; E=1.02; R=19.70; rawP=2.58e-22; adjP=6.90e-22
IGF1 pathway	20	P08700P01375P01137P14780P13500P01160P03956Q99988P36897P22301P13501P09237P29279P01033P08254P09603P05231P08253Q53ZZ1P02741	C=1291; O=20; E=1.02; R=19.65; rawP=2.70e-22; adjP=6.90e-22
Class I PI3K signaling events mediated by Akt	20	P08700P01375P01137P14780P13500P01160P03956Q99988P36897P22301P13501P09237P29279P01033P08254P09603P05231P08253Q53ZZ1P02741	C=1288; O=20; E=1.02; R=19.70; rawP=2.58e-22; adjP=6.90e-22
mTOR signaling pathway	20	P08700P01375P01137P14780P13500P01160P03956Q99988P36897P22301P13501P09237P29279P01033P08254P09603P05231P08253Q53ZZ1P02741	C=1288; O=20; E=1.02; R=19.70; rawP=2.58e-22; adjP=6.90e-22
Integrin family cell surface interactions	21	P08700P01375P01137P14780P13500P01160P03956Q99988P36897P22301P13501P00750P09237P29279P01033P08254P09603P05231P08253Q53ZZ1P02741	C=1378; O=21; E=1.09; R=19.33; rawP=2.12e-23; adjP=6.90e-22
ErbB receptor signaling network	20	P08700P01375P01137P14780P13500P01160P03956Q99988P36897P22301P13501P09237P29279P01033P08254P09603P05231P08253Q53ZZ1P02741	C=1312; O=20; E=1.03; R=19.34; rawP=3.72e-22; adjP=6.92e-22
Sphingosine 1-phosphate (S1P) pathway	20	P08700P01375P01137P14780P13500P01160P03956Q99988P36897P22301P13501P09237P29279P01033P08254P09603P05231P08253Q53ZZ1P02741	C=1311; O=20; E=1.03; R=19.35; rawP=3.66e-22; adjP=6.92e-22
TRAIL signaling pathway	20	P08700P01375P01137P14780P13500P01160P03956Q99988P36897P22301P13501P09237P29279P01033P08254P09603P05231P08253Q53ZZ1P02741	C=1328; O=20; E=1.05; R=19.10; rawP=4.72e-22; adjP=8.55e-22
Glypican pathway	20	P08700P01375P01137P14780P13500P01160P03956Q99988P36897P22301P13501P09237P29279P01033P08254P09603P05231P08253Q53ZZ1P02741	C=1338; O=20; E=1.05; R=18.96; rawP=5.47e-22; adjP=9.64e-22
Proteoglycan syndecan-mediated signaling events	20	P08700 P01375 P0 1137 P14780 P13 500 P01160 P03956 Q9998 8 P36897 P22 301P13501 P09237 P29279 P01033 P0 8254 P09603 P05231 P0 8253 Q53ZZ1 P02741	C=1345; O=20; E=1.06; R=18.86; rawP=6.06e-22; adjP=1.04e-21

Beta1 integrin cell surface interactions	20	P08700P01375P01137P14780P13500P01160P03956Q99988P36897P22301P13501P09237P29279P01033P08254P09603P05231P08253Q53ZZ1P02741	C=1351; O=20; E=1.07; R=18.78; rawP=6.62e-22; adjP=1.11e-21
AP-1 transcription factor network	15	P08700P01375P01137P14780P13500P01160P03956P36897P22301P01033P29279P05231P08253Q53ZZ1P02741	C=623; O=15; E=0.49; R=30.54; rawP=3.03e-19; adjP=4.95e-19
Integrin-linked kinase signaling	15	P08700P01375P01137P14780P13500P01160P03956P36897P22301P01033P29279P05231P08253Q53ZZ1P02741	C=656; O=15; E=0.52; R=29.00; rawP=6.55e-19; adjP=1.04e-18
CDC42 signaling events	15	P08700P01375P01137P14780P13500P01160P03956P36897P22301P01033P29279P05231P08253Q53ZZ1P02741	C=757; O=15; E=0.60; R=25.13; rawP=5.50e-18; adjP=8.57e-18
Regulation of CDC42 activity	15	P08700P01375P01137P14780P13500P01160P03956P36897P22301P01033P29279P05231P08253Q53ZZ1P02741	C=770; O=15; E=0.61; R=24.71; rawP=7.07e-18; adjP=1.08e-17
Validated transcriptional targets of AP1 family members Fra1 and Fra2	8	P08700P01375P14780P13500P03956P05231P08253Q53ZZ1	C=136; O=8; E=0.11; R=74.61; rawP=1.34e-13; adjP=2.00e-13
amb2 Integrin signaling	6	P01375P14780P00750P29279P05231P08253	C=41; O=6; E=0.03; R=185.63; rawP=6.64e-13; adjP=9.67e-13
IL12-mediated signaling events	6	P01375P01137Q14116P05231Q53ZZ1P10147	C=113; O=6; E=0.09; R=67.35; rawP=3.58e-10; adjP=5.10e-10
IL27-mediated signaling events	4	P01375P01137Q14116P05231	C=26; O=4; E=0.02; R=195.14; rawP=4.75e-09; adjP=6.63e-09
ALK1 signaling events	7	P08700P01375P01137P36897P22301P29279Q53ZZ1	C=321; O=7; E=0.25; R=27.66; rawP=5.37e-09; adjP=7.34e-09
ALK1 pathway	7	P08700P01375P01137P36897P22301P29279Q53ZZ1	C=324; O=7; E=0.26; R=27.40; rawP=5.72e-09; adjP=7.66e-09
TGF-beta receptor signaling	6	P08700P01375P36897P22301P29279Q53ZZ1	C=305; O=6; E=0.24; R=24.95; rawP=1.36e-07; adjP=1.72e-07
Regulation of nuclear SMAD2/3 signaling	6	P08700P01375P36897P22301P29279Q53ZZ1	C=305; O=6; E=0.24; R=24.95; rawP=1.36e-07; adjP=1.72e-07
Regulation of cytoplasmic and nuclear SMAD2/3 signaling	6	P08700P01375P36897P22301P29279Q53ZZ1	C=305; O=6; E=0.24; R=24.95; rawP=1.36e-07; adjP=1.72e-07
Peptide ligand-binding receptors	5	Q9ULZ1P13500P13501P10147P01185	C=167; O=5; E=0.13; R=37.98; rawP=2.08e-07; adjP=2.58e-07
IL23-mediated signaling events	4	P01375P13500Q14116P05231	C=66; O=4; E=0.05; R=76.88; rawP=2.24e-07; adjP=2.73e-07
LPA receptor mediated events	4	P01375P14780P05231P08253	C=100; O=4; E=0.08; R=50.74; rawP=1.20e-06; adjP=1.44e-06
Class A/1 (Rhodopsin-like receptors)	5	Q9ULZ1P13500P13501P10147P01185	C=276; O=5; E=0.22; R=22.98; rawP=2.47e-06; adjP=2.90e-06
Signal Transduction	8	P01137P14780Q9ULZ1P13500P36897P13501P10147P01185	C=1231; O=8; E=0.97; R=8.24; rawP=4.04e-06; adjP=4.67e-06
GPCR ligand binding	5	Q9ULZ1 P13500 P13501 P10147 P01185	C=338; O=5; E=0.27; R=18.76; rawP=6.63e-06; adjP=7.53e-06
CXCR4-mediated signaling events	4	P08700P01375P14780Q53ZZ1	C=192; O=4; E=0.15; R=26.43; rawP=1.59e-05; adjP=1.78e-05
Posttranslational regulation of adherens junction stability and dissassembly	4	P14780P09237P08254P08253	C=231; O=4; E=0.18; R=21.96; rawP=3.28e-05; adjP=3.60e-05
N-cadherin signaling events	4	P14780P09237P08254P08253	C=251; O=4; E=0.20; R=20.21; rawP=4.53e-05; adjP=4.90e-05
E-cadherin signaling in the nascent adherens junction	4	P14780P09237P08254P08253	C=275; O=4; E=0.22; R=18.45; rawP=6.45e-05; adjP=6.75e-05
Stabilization and expansion of the E-cadherin adherens junction	4	P14780P09237P08254P08253	C=275; O=4; E=0.22; R=18.45; rawP=6.45e-05; adjP=6.75e-05
E-cadherin signaling events	4	P14780P09237P08254P08253	C=280; O=4; E=0.22; R=18.12; rawP=6.92e-05; adjP=7.13e-05
(C) WikiPathways			
Matrix Metalloproteinases	10	P01375P14780P16035P09237P08254P01033P22894P08253Q99727P03956	C=31; O=10; E=0.02; R=409.17; rawP=9.39e-25; adjP=1.31e-23
TWEAK Signaling Pathway	5	P01375P14780P13500P05231P13501	C=56; O=5; E=0.04; R=113.25; rawP=8.31e-10; adjP=5.82e-09
Cytokines and Inflammatory Response	5	P01375P01137P09603P05231P22301	C=67; O=5; E=0.05; R=94.66; rawP=2.09e-09; adjP=9.75e-09
Integrated Pancreatic Cancer Pathway	6	P08700P01375P01137P02729Q53ZZ1P36897	C=181; O=6; E=0.14; R=42.05; rawP=6.13e-09; adjP=2.15e-08
Selenium Pathway	5	P01375P13500P05231P00750P02741	C=108; O=5; E=0.09; R=58.72; rawP=2.36e-08; adjP=6.61e-08
Senescence and Autophagy	5	P08700P01137P05231P10147P00750	C=120; O=5; E=0.09; R=52.85; rawP=4.00e-08; adjP=9.33e-08
Angiogenesis overview	4	P14780P16035P08253Q99727	C=79; O=4; E=0.06; R=64.22; rawP=4.64e-07; adjP=9.28e-07
Oncostatin M Signaling Pathway	4	P08254P01033P13500P03956	C=85; O=4; E=0.07; R=59.69; rawP=6.23e-07; adjP=1.09e-06
MicroRNAs in cardiomyocyte hypertrophy	4	P01375P01137P01160P16860	C=103; O=4; E=0.08; R=49.26; rawP=1.35e-06; adjP=2.10e-06
Toll-like receptor signaling pathway	4	P01375P05231P10147P13501	C=116; O=4; E=0.09; R=43.74; rawP=2.16e-06; adjP=3.02e-06
Adipogenesis	4	P01375P01137P05231Q15848	C=130; O=4; E=0.10; R=39.03; rawP=3.41e-06; adjP=4.34e-06

Regulation of toll-like receptor signaling pathway	4	P01375P05231P10147P13501	C=154; O=4; E=0.12; R=32.95; rawP=6.67e-06; adjP=7.78e-06
MAPK signaling pathway	4	P01375P01137Q53ZZ1P36897	C=165; O=4; E=0.13; R=30.75; rawP=8.76e-06; adjP=9.43e-06
SIDS Susceptibility Pathways	4	P01375P05231P22301P01185	C=214; O=4; E=0.17; R=23.71; rawP=2.43e-05; adjP=2.43e-05

[a]Number of submitted proteins involved in the pathway
[b]Accession number in Swiss-Prot Protein database
[c]Statistics column lists: C=the number of reference genes in the category; O=the number of proteins in the gene set and also in the category; E= the expected number in the category; R=ratio of enrichment; rawP= *p* value from the Fisher exact test; adjP=*p* value adjusted for multiple testing.

Table 3: Functional enriched categories inBPLVR list supplied by ProfCom_GO (short summary).

GO term	Description	I^A	I^B	*p*-value
Enriched categories of degree 0				
GO:0022617	EXTRACELLULAR MATRIX DISASSEMBLY	8 (34)	29 (17987)	3.60e-13
GO:0005576	EXTRACELLULAR REGION	27 (34)	1487 (17987)	1.81e-20
GO:0005615	EXTRACELLULAR SPACE	25 (34)	811 (17987)	7.12e-24
GO:0001666	RESPONSE TO HYPOXIA	9 (34)	163 (17987)	1.84e-08
Enriched categories of degree 1				
(GO:0022617 and GO:0005576)	(EXTRACELLULAR MATRIX DISASSEMBLY andEXTRACELLULAR REGION)	8 (34)	23 (17987)	5.36e-11
(GO:0005615 and GO:0001666)	(EXTRACELLULAR SPACE and RESPONSE TO HYPOXIA)	9 (34)	42 (17987)	6.88e-11
Enriched categories of degree 2				
(GO:0022617 and GO:0005576 not GO:0031012)	((EXTRACELLULAR MATRIX DISASSEMBLY and EXTRACELLULAR REGION) not EXTRACELLULAR MATRIX)	8 (34)	18 (17987)	2.07-09
(GO:0005615 and GO:0001666 not GO:0030154)	((EXTRACELLULAR SPACE and RESPONSE TO HYPOXIA) not CELL DIFFERENTIATION))	9 (34)	37 (17987)	8.32e-09
Enriched categories of degree 3				
(GO:0022617 and GO:0005576 not GO:0031012 not GO:0007586)	(((EXTRACELLULAR MATRIX DISASSEMBLY and EXTRACELLULAR REGION) notEXTRACELLULAR MATRIX) not DIGESTION)	8 (34)	15 (17987)	9.90e-08
(GO:0022617 notGO:0031012 and GO:0005576 not GO:0007586)	(((EXTRACELLULAR MATRIX DISASSEMBLY not EXTRACELLULAR MATRIX) and EXTRACELLULAR REGION) not DIGESTION)	8 (34)	15 (17987)	9.90e-08
(GO:0022617 notGO:0031012 not GO:0005886 and GO:0030198)	(((EXTRACELLULAR MATRIX DISASSEMBLYnot EXTRACELLULAR MATRIX) not PLASMA MEMBRANE) andEXTRACELLULAR MATRIX ORGANIZATION)	8 (34)	16 (17987)	1.98e-07

I^A=The number of proteins from the input list classified by the GO term (in brackets the size of the input list is reported);
I^B=The total number of genes in the whole genome classified by the GO term (in brackets the number of genes in the whole genome is given).
By using Bonferroni correction or Monte-Carlo simulations the *p*-value of the enrichment is adjusted.

rheumatoid arthritis (10 proteins of the input list) and cancer (7 proteins), in addition to a remarkable involvement of proteins related to cytokine-cytokine receptor interaction (12 proteins). The outcomes obtained withPathwayCommonsdatabase reinforced the previous results, underlining a strong activation of intracellular signaling cascadestriggered by cytokines and growth factors, as well as the opening of pathways involved in cell migration (Arf6, focal adhesion kinase and nestin). By using the Wikipathway platform,we obtained a significant enrichment of'matrix metalloproteinases' (10 proteins of the input list),'cytokines and inflammatory response' (5 proteins) and, interestingly, of'TWEAK signaling pathway'. TNF related weak inducer of apoptosis (TWEAK) is a small pleiotropic cytokine of the TNF super family. The multiple biological activities of TWEAK include stimulation of cell growth and angiogenesis, induction of inflammatory cytokines, and stimulation of apoptosis.

GO functional enrichments

The submission of the blood protein list to the BioProfiling platform revealed statistically significant functional enrichments by using ProfCom_GO. Table 3 provides a short summary of ProfCom_GO output Table. Categories of degree 0 correspond to single GO term, while categories of degree 1, 2 and 3 are obtained by combining pair, triplet, and quadruplet of GO terms, respectively. The main enrichments concerned proteins involved in 'extracellular region', 'response to hypoxia', 'inflammatory response'and 'protein binding'(see Table S3 for full report).Among the enriched categories of degree 0 reported in Table 3, the GO terms 'extracellular matrix disassembly'and 'extracellular region' identified 8 and 26 proteins of input list (IA), respectively. In the human whole genome (IB), the proteins classified according these GO termswere29 for 'extracellular matrix disassembly'and 1487 for 'extracellular region'. By combining two functional categories (degree 1), the number of identified proteins in submitted list remained the same but in the whole genome only 23 proteins belonged to this class. The complex function 'extracellular matrix disassembly AND extracellular region EXCLUDING extracellular matrix EXCLUDING digestion'supplied by ProfCom (degree 3) was even more specific, since only 15 genes in the human whole genome were classified by this complex function. The 8 proteins of input list related by this function complex were:MMP-1, MMP-2, MMP-3, MMP-7, MMP-8, MMP-9, TIMP-1, and TIMP-2.

Similarly, by combining the GO annotations'extracellular space AND response to hypoxia'(degree 1), we related9 proteins from input list(CRP, IL-18, MMP-9, BNP, t-PA, MCP-1, TGF-β1, TNF-α, and adiponectin) and 42in the whole genome. In whole human genome, by considering the single GO annotations, the program identifies 811proteins with the term 'extracellular space'and 163proteins with the annotation 'response to hypoxia'.

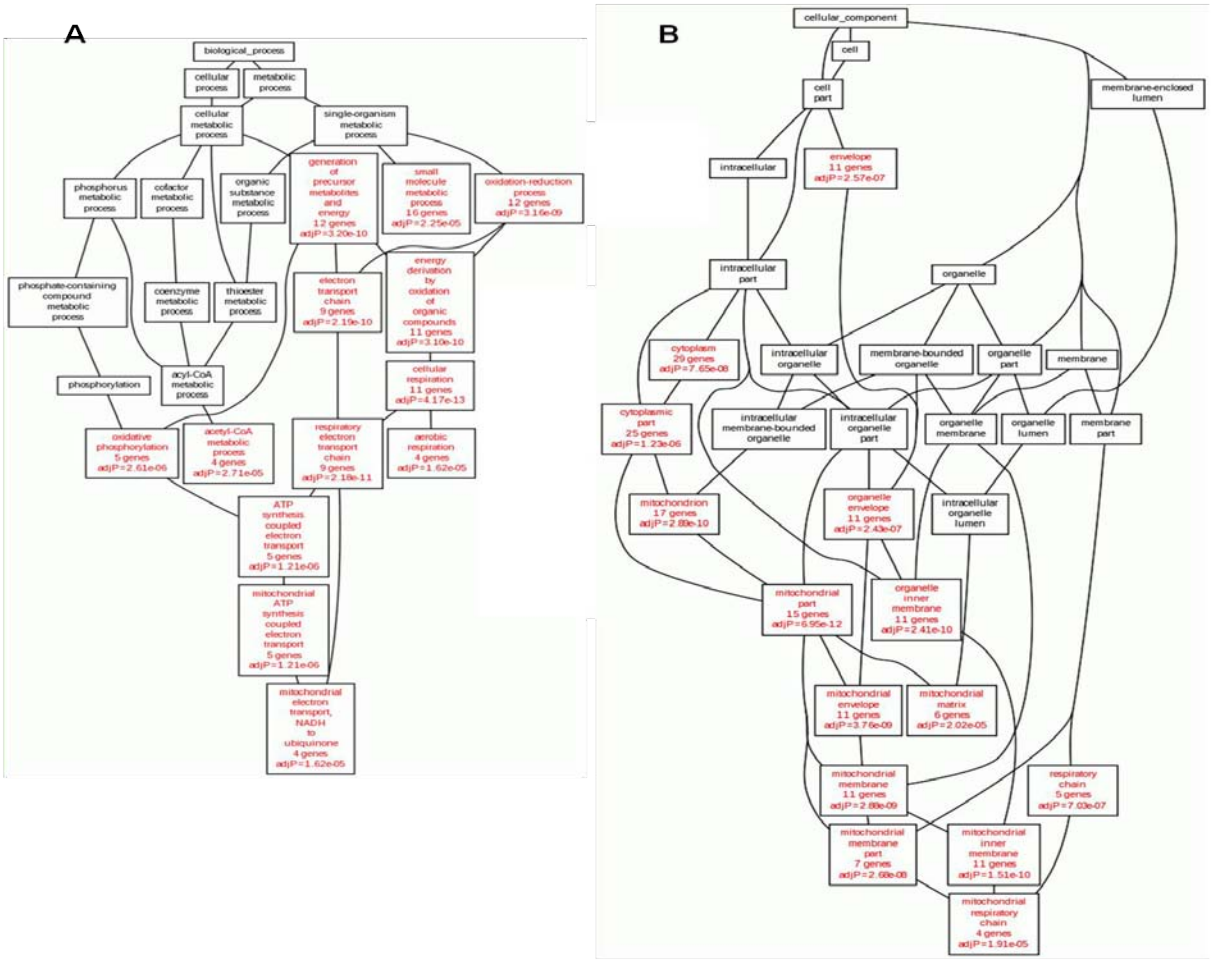

Figure 2: Over-representation analysis of GO categories in LVTP. The analysis with WebGestalt disclosed functional GO enrichments grouped according to Biological Process (A), and Cellular Component (B). GO terms in red are the enriched GO categories while the black ones are their non-enriched parents. Each node shows the name of the GO category, the number of genes in the category and the adjusted p-value indicating the significance of enrichment.

Bioinformatics analysis of the LV tissue proteins list from patients with HF (LVTP)

The proteomic study in cardiac tissue from patients with HFevaluated by Roselló-Lletí[36]was used in this work and the LV protein list found differentially regulated in ICM patients (Table S1) was uploaded into the WebGestalt portal to perform ORA. Then, by using BioProfiling devices, we enriched the input list in terms of a network-based statistical framework. Finally, we again investigated the enriched protein-protein interactions networks provided by R and PPI spiders by WebGestal.

GO over-representation analysis

Figure 2 shows the significant GO enrichments obtained in BPand CC area(Panels A and B, respectively) following the submission of LV protein list into theWebGestalt platform. No statistically significant enrichmentwas providedwith GO MF terms. TheBP enriched classes revealed that the majority of the submitted proteins were involved in 'cellular respiration' (GO:0045333 - 11 proteins), electron transport chain and ATP production ('mitochondrial ATP synthesis coupled electron transport' - GO:0042775 - 5 proteins), and metabolism ('acetylCoA metabolic process' – GO:0006084 – 4 proteins). Theenrichment analysis in CC area confirmed that more than 50% of the submitted proteins localized in the 'mitochondrion' (GO: 0005739 –17 proteins). 6 of these were proteins of the 'mitochondrial matrix' (GO:0005759), while 11 were associated to the 'mitochondrial inner membrane' (GO:0005743). More in details, 4proteins were part of the 'mitochondrial respiratory chain' (GO:0005746). The full report of enriched GO categories provided by WebGestaltis available in supplementary information (Table S4).

The LV protein set was then explored by KEGG, PathwayCommons and Wikipathways databases. The outcomes supplied by these bioinformatics devices further supported a remarkable involvement of pathways associated to electron transport chain, oxidative phosphorilation, and metabolism, with strong activation of the Krebs cycle (data not shown).

GO functional enrichments

In Bioprofiling, we obtained significant enrichments with ProfCom_GO (Table S5), PPI and R spider tools. The analysis of the networks provided by both spider applications may be deeply helpful to identify new proteins not previously associated with the disease and, accordingly, to develop newhypotheses regarding putative

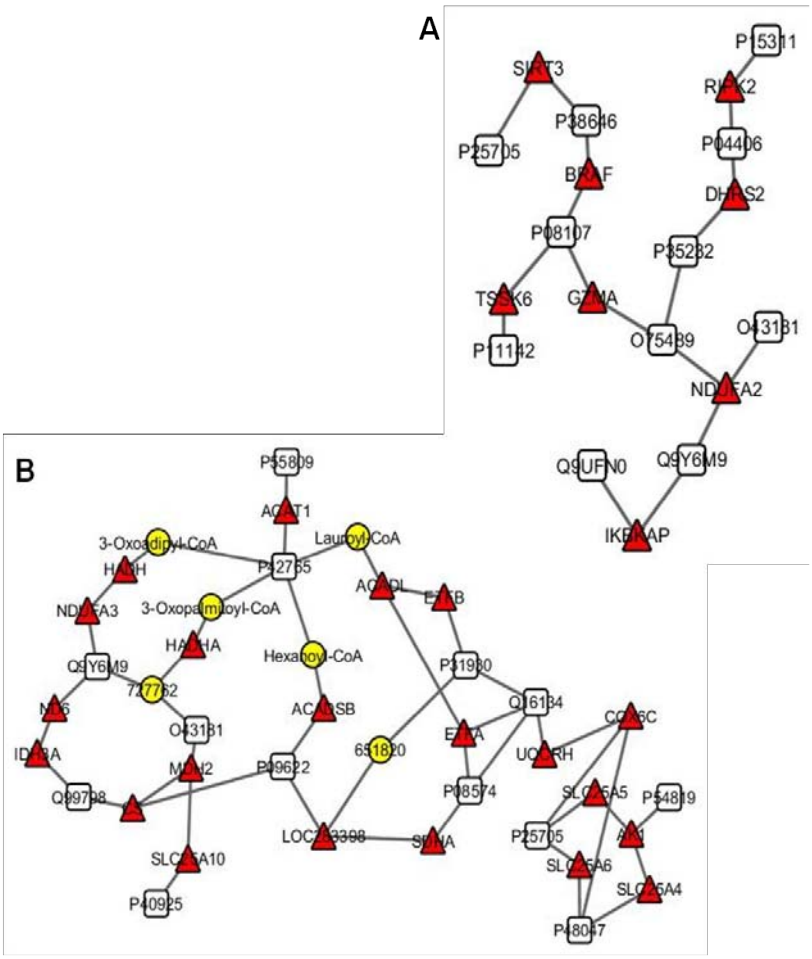

Figure 3: Results obtained by BioProfiling analysis following the submission of LVTP. (A), Graphic illustration of PPI spider's model D2, in which is addedone intermediate node to the protein network. (B), Graphic illustrations of R spider's model D3, in which are added two intermediate nodes to the protein network. In both network the nodes arising from the input list are shown as white squares, whereas the intermediate nodes are represented by red triangles. The edges represent the interactions among the protein nodes. The yellow circles in panel B indicate the metabolites involved in metabolic and signaling pathways.

prognostic indicators which may subsequently be validated.

In Figure 3 are illustrated the outcomes by PPI spider (Panel A) and R spider (Panel B). The graphical illustrations of the models were obtained with Cytoscape 3.1. Concerning the analysis with PPI spider, we acquired only model D2 (one intermediate allowed), that involved 11proteins of submitted list, 8 new intermediate proteins, and 36 interacting protein pairs, with a p-value < 0.005. Among theintermediate nodes, the protein that showed the highest number of interactionswas the NADH dehydrogenase (ubiquinone) 1 alpha sub-complex 2 (NDUFA2). The PPI network D2 reinforced the enrichment of proteins associated with the inflammatory response showing as intermediates some proteins involved in immune response[receptor-interacting serine-threonine kinase 2 ([RIPK2], granzyme A [GZMA] and IkappaB kinase complex-associated protein[IKBAP).

Figure 3, Panel Bshows the protein network obtained with respect tothe reference knowledge from Reactome and KEGG databases. Among the models supplied by R spider, we just considered the D3 network, covering 13 proteins from the input list and including 88 interacting protein pairs (p-value < 0.005). The inferred model contained also sixintracellular metabolites, represented in the network by yellow circles, and 21 intermediate nodes. Among the intermediate proteins, we found once againmitochondrial proteins involved in the respiratory chain, in ATP synthesis,and metabolism. Among the proteins provided by the enriched PPI network and missing in the input list, we disclosed specific proteins of the respiratory chain. In addition, the R spider's network highlighted a considerable participation of members of ATP/ADP mitochondrial carrier subfamily, like the ADP/ATP translocase 1, 2 and 3. The complete list of intermediate nodes engaged in both protein networks (PPI spider and R spider) is reportedin table S6.

GO over-representation analysis of the enriched networks

Following the generation of enriched networks by Bioprofiling, we created two novel protein lists by combining the LV proteinspreviously identifiedin failing hearts with the new intermediates proteinsrecognized by PPI and R spider tools. Accordingly, we obtained one set of 41 protein IDs adding the intermediate nodes identified by the model D2 of PPI spider, and one list of 54 LV proteins inserting the intermediates disclosed by the model D3 of R spider. The new input lists were separately submitted

Table 4: Over-representation analysis of GO terms in enriched PPI spider interacting network (A) and R spider interacting network (B) supplied by WebGestalt.

GO category [a]	ID [b]	# [c]	adjP [d]
(A) Enriched Model D2 PPI spider			
Biological Process			
Cellular respiration	GO:0045333	13	6.08e-15
Respiratory electron transport chain	GO:0022904	10	7.47e-12
Energy derivation by oxidation of organic compounds	GO:0015980	13	2.61e-11
Oxidation-reduction process	GO:0055114	15	4.26e-11
Generation of precursor metabolites and energy	GO:0006091	14	4.26e-11
Electron transport chain	GO:0022900	10	5.10e-11
ATP synthesis coupled electron transport	GO:0042773	6	1.20e-07
Mitochondrial ATP synthesis coupled electron transport	GO:0042775	6	1.20e-07
Oxidative phosphorylation	GO:0006119	6	3.11e-07
Mitochondrial electron transport, NADH to ubiquinone	GO:0006120	5	1.11e-06
Aerobic respiration	GO:0009060	5	1.13e-06
Molecular Function			
Oxidoreductase activity	GO:0016491	11	2.65e-05
NADH dehydrogenase activity	GO:0003954	4	2.82e-05
Catalytic activity	GO:0003824	27	2.82e-05
Oxidoreductase activity, acting on NADH or NADPH	GO:0016651	5	2.82e-05
NADH dehydrogenase (ubiquinone) activity	GO:0008137	4	2.82e-05
NADH dehydrogenase (quinone) activity	GO:0050136	4	2.82e-05
Oxidoreductase activity, acting on NADH or NADPH, quinine or similar compound as acceptor	GO:0016655	4	7.36e-05
Cellular Component			
Mitochondrial part	GO:0044429	17	1.24e-12
Mitochondrion	GO:0005739	20	4.27e-11
Mitochondrial inner membrane	GO:0005743	12	7.10e-11
Organelle inner membrane	GO:0019866	12	1.37e-10
Mitochondrial membrane	GO:0031966	12	2.80e-09
Mitochondrial envelope	GO:0005740	12	3.79e-09
Mitochondrial membrane part	GO:0044455	8	4.44e-09
Organelle envelope	GO:0031967	13	3.16e-08
Cytoplasm	GO:0005737	35	3.16e-08
Envelope	GO:0031975	13	3.43e-08
Respiratory chain	GO:0070469	6	5.09e-08
Cytoplasmic part	GO:0044444	30	4.01e-07
Mitochondrial respiratory chain	GO:0005746	5	1.23e-06
Mitochondrial matrix	GO:0005759	7	5.64e-06
Mitochondrial respiratory chain complex I	GO:0005747	4	7.53e-06
NADH dehydrogenase complex	GO:0030964	4	7.53e-06
Respiratory chain complex I	GO:0045271	4	7.53e-06
Intracellular part	GO:0044424	36	1.77e-05
Intracellular	GO:0005622	36	4.34e-05
(B) Enriched Model D3 R spider			
Biological Process			
Cellular respiration	GO:0045333	21	2.78e-27
Oxidation-reduction process	GO:0055114	29	2.78e-27
Energy derivation by oxidation of organic compounds	GO:0015980	24	2.39e-27
Generation of precursor metabolites and energy	GO:0006091	25	7.54e-24
Respiratory electron transport chain	GO:0022904	16	2.70e-21
Electron transport chain	GO:0022900	16	3.25e-19
Small molecule metabolic process	GO:0044281	36	5.92e-17
Aerobic respiration	GO:0009060	9	3.50e-13
Tricarboxylic acid cycle	GO:0006099	7	3.93e-11
Acetyl-CoA catabolic process	GO:0046356	7	4.75e-11
Acetyl-CoA metabolic process	GO:0006084	8	9.69e-11
Coenzyme catabolic process	GO:0009109	7	1.88e-10

ATP synthesis coupled electron transport	GO:0042773	8	1.91e-10
Mitochondrial ATP synthesis coupled electron transport	GO:0042775	8	1.91e-10
Thioester metabolic process	GO:0035383	9	2.12e-10
Acyl-CoA metabolic process	GO:0006637	9	2.12e-10
Cofactor catabolic process	GO:0051187	7	4.70e-10
Oxidative phosphorylation	GO:0006119	8	6.31e-10
Mitochondrial electron transport, NADH to ubiquinone	GO:0006120	6	5.73e-08
Coenzyme metabolic process	GO:0006732	9	2.99e-07
Carboxylic acid metabolic process	GO:0019752	15	4.69e-07
Small molecule catabolic process	GO:0044282	9	1.23e-06
Single-organism catabolic process	GO:0044712	9	1.23e-06
Cofactor metabolic process	GO:0051186	9	1.23e-06
Carboxylic acid catabolic process	GO:0046395	8	1.86e-06
Organic acid catabolic process	GO:0016054	8	1.86e-06
Oxoacid metabolic process	GO:0043436	15	1.86e-06
Dicarboxylic acid metabolic process	GO:0043648	6	2.03e-06
Organic acid metabolic process	GO:0006082	15	2.05e-06
Cellular metabolic process	GO:0044237	44	3.32e-06
Fatty acid beta-oxidation	GO:0006635	5	7.91e-06
Metabolic process	GO:0008152	45	1.93e-05
Fatty acid catabolic process	GO:0009062	5	2.93e-05
Single-organism metabolic process	GO:0044710	44	4.17e-05
Lipid modification	GO:0030258	6	4.61e-05
Monocarboxylic acid catabolic process	GO:0072329	5	6.10e-05
Fatty acid oxidation	GO:0019395	5	6.10e-05
Cellular catabolic process	GO:0044248	17	6.74e-05
Lipid oxidation	GO:0034440	5	6.79e-05
Phosphorus metabolic process	GO:0006793	21	7.59e-05
Molecular Function			
Oxidoreductase activity	GO:0016491	21	4.84e-14
Coenzyme binding	GO:0050662	11	3.40e-10
Cofactor binding	GO:0048037	11	8.98e-09
Flavin adenine dinucleotide binding	GO:0050660	6	1.42e-06
NADH dehydrogenase (ubiquinone) activity	GO:0008137	5	2.09e-06
NADH dehydrogenase (quinone) activity	GO:0050136	5	2.09e-06
NADH dehydrogenase activity	GO:0003954	5	2.09e-06
NAD binding	GO:0051287	5	3.12e-06
Oxidoreductase activity, acting on NADH or NADPH	GO:0016651	6	3.12e-06
Catalytic activity	GO:0003824	34	5.45e-06
Oxidoreductase activity, acting on NADH or NADPH, quinine or similar compound as acceptor	GO:0016655	5	5.45e-06
Electron carrier activity	GO:0009055	6	4.68e-05
Hydrogen ion transmembrane transporter	GO:0015078	5	7.19e-05
Cellular Component			
Mitochondrial part	GO:0044429	33	5.82e-32
Mitochondrial inner membrane	GO:0005743	23	6.00e-25
Mitochondrion	GO:0005739	35	6.00e-25
Organelle inner membrane	GO:0019866	23	2.95e-24
Mitochondrial membrane	GO:0031966	24	4.60e-23
Mitochondrial envelope	GO:0005740	24	1.05e-22
Organelle envelope	GO:0031967	24	2.67e-18
Envelope	GO:0031975	24	3.35e-18
Mitochondrial matrix	GO:0005759	16	1.93e-16
Mitochondrial membrane part	GO:0044455	12	3.89e-14
Cytoplasmic part	GO:0044444	45	1.16e-13
Cytoplasm	GO:0005737	49	2.07e-13
Respiratory chain	GO:0070469	9	3.03e-12
Mitochondrial respiratory chain	GO:0005746	8	6.95e-11

Organelle membrane	GO:0031090	26	3.67e-10
Intracellular organelle part	GO:0044446	40	5.52e-09
Organelle part	GO:0044422	40	8.11e-09
Intracellular part	GO:0044424	49	2.44e-07
Mitochondrial respiratory chain complex I	GO:0005747	5	4.93e-07
NADH dehydrogenase complex	GO:0030964	5	4.93e-07
Respiratory chain complex I	GO:0045271	5	4.93e-07
Intracellular	GO:0005622	49	7.28e-07
Membrane-bounded organelle	GO:0043227	43	4.57e-06
Intracellular membrane-bounded	GO:0043231	43	4.57e-06
Intracellular organelle	GO:0043229	44	3.39e-05
Organelle	GO:0043226	44	3.42e-05

[a] Name of the enriched GO category
[b] GO category ID
[c] Number of input protein in the category
[d] Adjusted p value of enrichment

to WebGestalt and the bioinformatics analysis was limited to enriched GO categories. The results obtained were elaborated and summarized in table 4. The full reports of GO categories in enriched PPI and R spider networks are available in supplementary material (Table S7, S8). Analyzing the enriched networks, it was possible to better describe the molecular mechanisms which underlie the failure status. The predominant MFcategory was catalytic activity (27/34 proteins in PPI network and 34/54 proteins in R network). In particular, 11/34 proteins in the PPI network and 21/54 proteins in the R networkwere associated to oxidoreductase activity that involve NADH or NADPH as electron carrier. Moreover, the analysis of protein networks with two intermediate nodes showed asignificant enrichment of the multi-protein complex Iof the respiratory chain proteins.Finally, we demonstrated that the considerable increase of energy production mainly arose from carboxylic acid catabolic processes, and from the citric acid cycle.

Conclusions

The main purpose of this study was to use a systems biology approach for proposing novel hypothesis on mechanisms of LV remodeling and HF. The most significant findings of this study were: (i) blood analysis of early remodeling disclosed enrichments for ECM, stress response, response to hypoxia and inflammatory response,(ii) LV samples from end stage HF showed enrichments for respiratory chain, ATP production, and lipid metabolism, with deeply activation of the citric acid cycle.

As many authors reported, within a few hours following MI the release of pro-inflammatory cytokines stimulates the chemotaxis of the neutrophils into the injured zone.Subsequently the neutrophils draw the macrophages,which phagocyte the necrotic cardiomyocytes[37]. Moreover, during the inflammatory response to MI, a strong increase of the synthesis and the secretion of both matrix metalloproteinases and their tissue inhibitorsoccur. The net balance between these two systems coordinates the wound healing by helping the disposal of necrotic myocytes and the activation of myofibroblasts to initiate new ECM deposition to form the infarct scar [38].

The progression of LV remodeling into HF is the result of the loss of myocytes and maladaptive changes in the surviving myocytes and ECM. In our systems biology analysis, we highlighted an enrichment of ECM, cytokines and the inflammatory response. These results are in good accordance with the post-MI knowledge map recently published by Nguyen et al. [39]. Pro-inflammatory cytokines are expressed in all myocardial cells and have structural and functional consequences on the post-MI myocardium. Inflammatory mediators alone can induce several components in the HF pathway, including LV dysfunction, pulmonary edema, cardiomyopathy, endothelial dysfunction, cachexia/anorexia, adenylatecyclase receptor uncoupling, activation of the fetal gene program, and cardiac myocyte apoptosis [40]. In addition, alterations in the cardiac metabolism are key factors in the transition to HF. By analyzing the ORA of the enriched networks from PPI and R spider, we found an elevated involvement of protein interactions and metabolic pathways linked to an alteration of the mitochondrial function.Gupteand co-workerssuggested a global reduction in substrate oxidation,by finding reduced Krebs cycle intermediates[41]. These results were associated with decreased transcript levels for enzymes that catalyze fatty acid oxidation and pyruvate metabolism. Moreover,Karamanlidisand colleagues found out that mitochondrial respiratory dysfunction is linked to the pathogenesis of HF, predisposing the heart to injury by redox-sensitive mechanisms[42].

Systems biology is an emerging field of biomedical research that aims to understand the properties of a biological system by investigating the interrelationships and the interactions among its molecular components, such as genes, proteins and metabolites [44].The central point of this new research approach is identify the maps of such interactions using systematic and standardized approaches and assays that are unbiased as possible [45]. To date, the basic ideas of systems and network biology are already experimentally tested and applied to relevant biological problems, remarkably to multi-factorial diseases with complex etiologies. In the field of cardiovascular disease,Diez and colleagues have recently published a combined gene association and correlation network of atherosclerosis by performing systems biology analysis on data collected from47microarray [46].Isserlinand coworkers, by proteomic profiling and enriched maps, granted a more comprehensiveunderstanding of the progressive alterations associated with functional decline in dilatedcardiomyopathy in mouse model[47]. Finally, an unbiased systems approach was published to define energy metabolic events that occur in mouse model during the pathological cardiac remodeling and early stage of HF [48].

To date, adverse LV remodeling following MI still remains

difficult to distinguish from the normal wound healing repair, and HF is often discovered late during disease progression at a time when it is difficult to intervene. Based on this evaluation, future studies should evaluate whether early changes in ECM can predict later changes in cardiac metabolism. One limitation of this study was the inability to compare the early changes in the blood to late changes in the LV, due to differences in sampling types. Future studies will be needed to show and compare the two compartments alterations, in order to identify blood biomarkers that reflect tissue status along the time continuum of disease.

Acknowledgement

This work was partially supported by grants from the Ministerodell'Universita' e dellaRicercaScientifica e Tecnologica [Grant No. 2003063257-006 to P. A. Modesti], from the University of Florence [Grant No. 239, 2001 to P.A. Modesti], from the San Antonio Cardiovascular Proteomics Center funded from NHLBI [HHSN 268201000036C (N01-HV-00244), and NIH R01 HL075360] to M.L. Lindsey.

References

1. Howlett JG, McKelvie RS, Arnold JM, Costigan J, Dorian P, Ducharme A, et al. Canadian Cardiovascular Society Consensus Conference guidelines on heart failure - 2008 update: best practices for the transition of care of heart failure patients, and the recognition, investigation and treatment of cardiomyopathies. Can J Cardiol 2008; 24: 21-40.
2. Korup E, Dalsgaard D, Nyvad O, Jensen TM, Toft E, et al. Comparisons of degrees of left ventricular dilation within 3 hours and up 6 days after onset of first acute myocardial infarction. Am J Cardiol 1997; 80:449-453.
3. Solomon SD, Glynn RJ, Greaves S, Ajani U, Rouleau JL, Menapace F, et al. Recovery of ventricular function after myocardial infarction in the reperfusion era: the healing and early afterload reducing therapy study. Ann Intern Med 2001; 134: 451- 458.
4. Remme WJ, Swedberg K. Task Force for the Diagnosis and Treatment of Chronic Heart Failure, European Society of Cardiology. Guidelines for the diagnosis and treatment of chronic heart failure. Eur Heart J 2001; 22: 1527-1560.
5. Wang TJ, Levy D, Benjamin EJ, Vasan RS. The epidemiology of "asymptomatic" left ventricular systolic dysfunction: implications for screening. Ann Intern Med 2003; 38: 907-916.
6. Liu YY, Slotine JJ, Barabási AL. Observability of complex systems. ProcNatlAcadSci USA 2013; 110: 2460-2465.
7. Piestrzeniewicz K, Luczak K, Maciejewski M, Drozdz J. Low adiponectin blood concentration predicts left ventricular remodeling after ST-segment elevation myocardial infarction treated with primary percutaneous coronary intervention. Cardiol J 2010; 17: 49-56.
8. Weir RA, Chonq KS, Dalzell JR, Petrie CJ, Murphy CA, et al. Plasma apelin concentration is depressed following acute myocardial infarction in man. Eur J Heart Fail 2009; 11: 551-558.
9. Yoshitomi Y, Nishikimi T, Kojima S, Kuramochi M, Takishita S, et al. Plasma natriuretic peptides as indicators of left ventricular remodeling after myocardial infarction. Int J Cardiol 1998; 64: 153-160.
10. Naqaya N, Nishikimi T, Goto Y, Miyao Y, Kobayashi Y, et al. Plasma brain natriuretic peptide is a biochemical marker for the prediction of progressive ventricular remodeling after acute myocardial infarction. Am Heart J 1998; 135: 21-28.
11. Fertin M, Bauters A, Pinet F, Bauters C. Circulating levels of soluble Fas ligand and left ventricular remodeling after acute myocardial infarction (from the REVE-2 study). J Cardiol 2012; 60: 93-97.
12. Dominguez-Rodriguez A, Abreu-Gonzalez P, Avanzas P. Relation of growth-differentiation factor 15 to left ventricular remodeling in ST-segment elevation myocardial infarction. Am J Cardiol 2011; 108: 955-958.
13. Weir RA, Balmain S, Steedman T, Ng LL, Squire IB, et al. Tissue plasminogen activator antigen predicts medium-term left ventricular end-systolic volume after acute myocardial infarction. J Thromb Thrombolysis 2010; 29: 421-428.
14. Parissis JT, Adamopoulos S, Venetsanou KF, Mentzikof DG, Karas SM, et al. Serum profiles of C-C chemokines in acute myocardial infarction: possible implication in postinfarction left ventricular remodeling. J Interferon Cytokine Res 2002; 22: 223-229.
15. Gravning J, Ørn S, Kaasbøll OJ, Martinov VN, Manhenke C, et al. Myocardial connective tissue growth factor (CCN2/CTFG) attenuates left ventricular remodeling after myocardial infarction. Plose One 2012; 7: e52120.
16. Karpiński Ł1, Płaksej R, Derzhko R, Orda A, Witkowska M. Serum levels of interleukin-6, interleukin-10 and C-reactive protein in patients with myocardial infarction treated with primary angioplasty during a 6-month follow-up. Pol Arch Med Wewn 2009; 119: 115-121.
17. Oren H, Erbay AR, Balci M, Cehreli S. Role of novel mediators of inflammation in left ventricular remodeling in patients with acute myocardial infarction: do they affect the outcome of patients? Angiology 2007; 58: 45-54.
18. Dominguez-Rodriguez A, Abreu-Gonzalez P, Arroyo-Ucar E, Avanzas P. Serum ferritin deficiency and major adverse cardiovascular events after primary percutaneous coronary intervention in patients with ST-elevation myocardial infarction without anemia. Int J Cardiol 2013; 168: 4914-4916.
19. Weir RA, Miller AM, Murphy GE, Clements S, Steedman T, et al. Serum soluble ST2: a potential novel mediator in left ventricular and infarct remodeling after acute myocardial infarction. J Am CollCardiol 2010; 55: 243-250.
20. Weinberg EO, Shimpo M, De Keulenaer GW, MacGillivray C, Tominaga S, et al. Expression and regulation of ST2, an interleukin-1 receptor family member, in cardiomyocytes and myocardial infarction. Circulation 2002; 106: 2961-2966.
21. Sabatine MS, Morrow DA, Higgins LJ, MacGillivray C, Guo W, et al. Complementary roles for biomarkers of biomechanical strain ST2 and N-terminal prohormone B-type natriuretic peptide in patients with ST-elevation myocardial infarction. Circulation 2008; 117: 1936-1944.
22. Welsh P, Woodward M, Rumley A, Lowe G. Associations of circulating TNF alpha and IL-18 with myocardial infarction and cardiovascular risk markers: the Glasgow Myocardial Infarction Study. Cytokine 2009; 47: 143-147.
23. Fertin M, Lemesle G, Turkieh A, Beseme O, Chwastyniak M, et al. Serum MMP-8:anovel Indicator of Left Ventricular Remodeling and Cardiac Outcome in Patients after Acute Myocardial Infarction. PLoS One 2013; 8:e71280.
24. Tziakas DN, Chalikias GK, Hatzinikolaou EI, Stakos DA, Tentes IK, et al. N-terminal Pro-B-Type Natriuretic Peptide and Matrix Metalloproteinases in Early and Late Left Ventricular Remodeling After Acute Myocardial Infarction. Am J Cardiol 2005; 96: 31-34.
25. Webb CS, Bonnema DD, Ahmed SH, Leonardi AH, McClure CD, et al. Specific temporal profile of matrix metalloproteinase release occurs in patients after myocardial infarction: relation to left ventricular remodeling. Circulation 2006; 114: 1020-1027.
26. Kelly D, Cockerill G, Ng LL, Thompson M, Khan S, et al. Plasma matrix metalloproteinase-9 and left ventricular remodeling after acute myocardial infarction in man: a prospective cohort study. Eur Heart J 2007; 28: 711-718.
27. Squire IB, Evans J, Ng LL, Loftus IM, Thompson MM. Plasma MMP-9 and MMP-2 following acute myocardial infarction in man: correlation with echocardiographic and neurohumoral parameters of left ventricular dysfunction. J Card Fail 2004; 10: 328-333.
28. Kelly D, Khan S, Cockerill G, Ng LL, Thompson M, et al. Circulating stromelysin-1 (MMP-3): a novel predictor of LV dysfunction, remodeling and all-cause mortality after acute myocardial infarction. Eur J Heart Fail 2008; 10: 133-139.
29. Dominguez-Rodriguez A, Abreu-Gonzalez P, Avanzas P, Laynez-Cerdeña I, Kaski JC. Neopterin predicts left ventricular remodeling in patients with ST-segment elevation myocardial infarction undergoing primary percutaneous coronary intervention. Athrosclerosis 2010; 211: 574-578.

30. Devaux Y, Bousquenaud M, Rodius S, Marie PY, Maskali F, et al. Transforming growth factor b receptor 1 is a new candidate prognostic biomarker after acute myocardial infarction. BMC Med Genomics 2011; 4: 83.

31. Khan SQ, Dhillon OS, O'Brien RJ, Struck J, Quinn PA, et al. C-terminal provasopressin (copeptin) as a novel and prognostic marker in acute myocardial infarction: Leicester Acute Myocardial Infarction Peptide (LAMP) study. Circulation 2007; 115: 2103-2110.

32. Kelly D, Squire IB, Khan SQ, Quinn P, Struck J, et al. C-terminal provasopressin (copeptin) is associated with left ventricular dysfunction, remodeling, and clinical heart failure in survivors of myocardial infarction. J Card Fail 2008; 14: 739-745.

33. Roselló-Lletí E, Alonso J, Cortés R, Almenar L, Martínez-Dolz L, et al. Cardiac proteome changes in ischaemic and dilated cardiomiopathy: a proteomic study of human left ventricular tissue. J Cell Mol Med 2012; 16: 2471-2486.

34. Wang J, Duncan D, Shi Z, Zhang B. WEB-based GEneSeTAnaLysis Toolkit (WebGestalt): update 2013. Nucleic Acids Res 2013; 41: W77-W83.

35. Antonov AV. BioProfiling.de: analytical web portal for high-throughput cell biology. Nucleic Acids Res 2011; 39: W323-W327.

36. Shannon P, Markiel A, Ozier O, Baliga NS, Wang JT, et al. Cytoscape: a software environment for integrated models of biomolecular interaction networks. Genome Res 2003; 13: 2498-2504.

37. Ma Y, Yabluchanskiy A, Lindsey ML. Neutrophil roles in left ventricular remodeling following myocardial infarction. Fibrogenesis Tissue Repair 2013; 6: 11.

38. Peterson JT, Li H, Dillon L, Bryant J. Evolution of matrix metalloprotease and tissue inhibitor expression during heart failure progression in the infarcted rat. Cardiovascular Res 2000; 46: 3.7-315.

39. Nguyen NT, Zhang X, Wu C, Lange RA, Chilton RJ, et al. Integrative Computational and Experimental Approaches to Establish a Post-Myocardial Infarction Knowledge Map. PLoSComputBiol 2014; 10: e1003472.

40. Lindsey ML. MMP induction and inhibition in myocardial infarction. Heart Fail Rev 2004; 9: 7-19.

41. Gupte AA, Hamilton DJ, Cordero-Reyes AM, Youker KA, Yin Z, et al. Mechanical unloading promotes myocardial energy recovery in human heart failure. CircCardiovasc Genet 2014; 7: 266-276.

42. Karamanlidis G, Lee CF, Garcia-Menendez L, Kolwicz SC Jr, Suthammarak W, et al. Mitochondrial complex I deficiency increases protein acetylation and accelerates heart failure. Cell Metab 2013; 18:239-50.

43. Gamberi T, Magherini F, Bini L, Messori L, Gabbiani C, et al. New Insights into the Molecular Mechanisms of Selected Anticancer Metal Compounds through Bioinformatic Analysis of Proteomic Data. J. Proteomics Bioinform. 2013; S6.

44. Wolkenhauer O. Systems biology: The reincarnation of systems theory applied in biology? Brief Bioinform 2001; 2:258-70.

45. Vidal M, Cusick ME, Barabási AL. Interactome networks and human disease. Cell 2011; 144:986-98.

46. Diez D, Wheelock AM, Goto S, Haeggström JZ, Paulsson-Berne G, et al. The use of network analyses for elucidating mechanisms in cardiovascular disease. MolBiosyst 2010; 6:289-304.

47. Isserlin R, Merico D, Alikhani-Koupaei R, Gramolini A, Bader GD, et al.Pathway analysis of dilated cardiomyopathy using global proteomic profiling and enrichment maps. Proteomics 2010; 10:1316-1327.

48. Lai L, Leone TC, Keller MP, Martin OJ, Broman AT, et al. Energy metabolic reprogramming in the hypertrophied and early stage failing heart: a multisystems approach. Circ Heart Fail 2014; 7:1022-1031.

Austin J Proteomics Bioinform & Genomics - Volume 2 Issue 1 - 2015
ISSN : 2471-0423 | www.austinpublishinggroup.com

Citation: Pietrovito L, Nguyen NT, Jin YF, Modesti PA, Lindsey ML and Modesti A. Interacting Network Analysis and Functional Profiling to Look Inside Adverse Ventricular Remodeling Post-Myocardial Infarction. Austin J Proteomics Bioinform & Genomics. 2015;2(1): 1007.